
INTEGRATION OF RADIOMICS AND TUMOR BIOMARKERS IN INTERPRETABLE MACHINE LEARNING MODELS

A PREPRINT

Lennart Brocki and Neo Christopher Chung
 Institute of Informatics, University of Warsaw, Poland

March 21, 2023

ABSTRACT

Despite the unprecedented performance of deep neural networks (DNNs) in computer vision, their practical application in the diagnosis and prognosis of cancer using medical imaging has been limited. One of the critical challenges for integrating diagnostic DNNs into radiological and oncological applications is their lack of interpretability, preventing clinicians from understanding the model predictions. Therefore, we study and propose the integration of expert-derived radiomics and DNN-predicted biomarkers in interpretable classifiers which we call *ConRad*, for computerized tomography (CT) scans of lung cancer. Importantly, the tumor biomarkers are predicted from a concept bottleneck model (CBM) such that once trained, our ConRad models do not require labor-intensive and time-consuming biomarkers. In our evaluation and practical application, the only input to ConRad is a segmented CT scan. The proposed model is compared to convolutional neural networks (CNNs) which act as a black box classifier. We further investigated and evaluated all combinations of radiomics, predicted biomarkers and CNN features in five different classifiers. We found the ConRad models using non-linear SVM and the logistic regression with the Lasso outperform others in five-fold cross-validation, although we highlight that interpretability of ConRad is its primary advantage. The Lasso is used for feature selection, which substantially reduces the number of non-zero weights while increasing the accuracy. Overall, the proposed *ConRad* model combines CBM-derived biomarkers and radiomics features in an interpretable ML model which perform excellently for the lung nodule malignancy classification.

Keywords deep learning · interpretability · explainability · concept bottleneck · radiomics · feature engineering

Cancer kills about 10 million people annually, as a leading cause of death worldwide. Lung cancer is the most prevalent type of cancer in the world [World Health Organization] and kills more patients than any other cancer in the United States [Centers For Disease Control And Prevention]. Individuals suspecting or suffering from cancer routinely undergo medical imaging acquisition using computed tomography (CT), positron emission tomography (PET), and others, whose data (e.g., pixels and voxels) are becoming increasingly larger and more complex. Despite deep neural networks having shown unprecedented performance in computer vision, their application to medical images in clinical routine has been limited Van der Laak et al. [2021], Miotto et al. [2018]. One of the most important issues is a lack of interpretable machine learning models and a domain-specific implementation whose prediction can be understood by and communicated to clinicians [Rudin et al., 2022].

To overcome this challenge in the context of lung nodule malignancy classification, we have developed and investigated an interpretable machine learning model called *ConRad* which combines concept bottleneck models (CBM), which predict tumor biomarkers, and radiomic features, which are based on expert-derived characterization of medical images (fig. 1). Both of these feature sets have the advantage that their meaning is clearly defined which enhances our model's transparency. Radiomics [Lambin et al., 2017, Yip and Aerts, 2016]. It has been shown to uncover cancer signatures that are visually indistinguishable for doctors and are able to identify cancer subtypes [Hatt et al., 2019]. On the other hand, deep neural networks (DNNs) may result in high performance classifiers or features, that are not understood or explainable by oncological experts. As a proof-of-concept, we applied and evaluated different aspects of ConRad using the LIDC-IDRI (Lung Image Database Consortium and Image Database Resource Initiative) dataset Armato III et al. [2011].

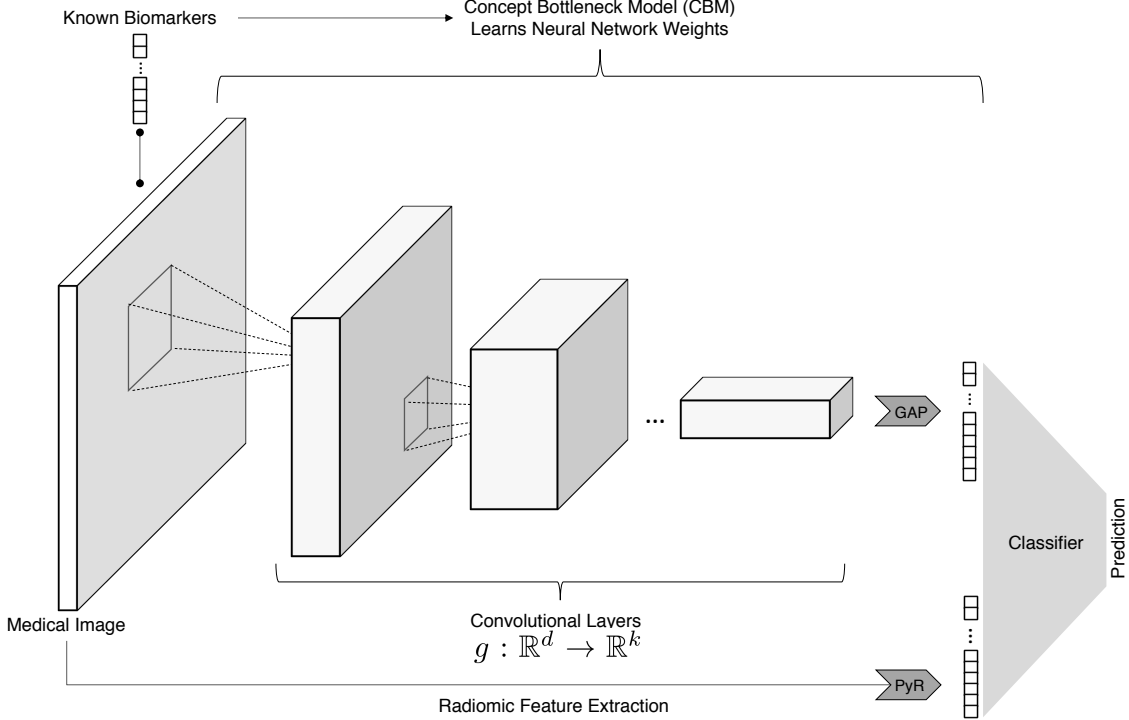


Figure 1: The proposed *ConRad* model integrates expert-derived radiomic features and biomarkers predicted from a concept bottleneck model (CBM) [Koh et al., 2020]. The final interpretable classifier uses both types of features competitively to classify a tumor as benign versus malignant.

Importantly, instead of using the annotated biomarkers directly in the malignancy prediction, we follow the concept bottleneck model (CBM) architecture [Koh et al., 2020] and train a DNN to predict the biomarkers which are then used in the final classifier. Therefore, once our model has been trained, biomarker annotations, which are expensive and time-consuming to obtain, are not needed anymore. Additionally, we perform standard radiomics feature extraction which provides interpretable statistical properties of cancer tumors. Both feature sets are fused to train the final classifier predicting benign vs. malignant tumors. Feature selection was explored by applying the Lasso (least absolute shrinkage and selection operator) [Tibshirani, 1996] to the logistic regression. The Lasso is shown to maintain, or even increase, the model performance while utilizing a substantially small number of features.

We have performed a comprehensive evaluation of various machine learning (ML) algorithms in ConRad models. Through 5-fold cross-validation, the performances are measured by the model accuracy, receiver operating characteristic (ROC) curves, and other metrics. On the other hand, we built end-to-end convolutional neural networks (CNNs), which directly predict the malignancy. From end-to-end CNNs, the CNN features are extracted and further used in independent ML classifiers for comparison. Both end-to-end CNNs and usage of CNN features represent uninterpretable black-box models, since radiologists do not gain any understanding about how the model is making its prediction. Our interpretable models perform comparable or superior to CNN.

There is an inherent trade-off between interpretability and accuracy in machine learning, including DNNs [Dziugaite et al., 2020]. Instead of hyper-optimizing DNN architectures on LIDC-IDRI data, our study aims to engineer inherently interpretable features that are based on well-established radiological and oncological expertises. In the next section 1, we summarize related works, focusing on the development of radiomics and DNNs for oncology. Our ConRad model, data, and evaluation, are detailed in section 2. Then section 3 shows performance metrics of different ML classifiers and comparison against black-box classifiers based on CNNs. We also demonstrate informative feature selection, automatically achieved through use of the Lasso. Lastly, we summarize our findings and provide concluding remarks in section 4.

1 Related Works

While the comprehensive review of DNNs applied on the lung nodule classification is beyond the scope of this paper, we note few related analysis of the LIDC-IDRI dataset Armato III et al. [2011]. Two of the earliest examples are Shen et al. [2015] and Kumar et al. [2015], which use a supervised multi-scale approach and unsupervised feature extraction via an auto-encoder, respectively. Other approaches include 3D CNNs, which have been used by [Zhu et al., 2018], so-called dilated CNN introduced in [Al-Shabi et al., 2019] and curriculum learning [Al-Shabi et al., 2022], where the model is first trained on easy and later on harder samples, progressively growing the network in the process. All these approaches have in common that they focus on improving model accuracy and do not consider the interpretability of the developed models.

Our model shares similarities with the methods employed in [Causey et al., 2018, Mehta et al., 2021, Shen et al., 2019], which all use features beyond the image pixels themselves. Radiomics features are combined with CNN features in Causey et al. [2018], but in contrast to ours, the annotated biomarkers are not used. The biomarkers are combined with CNN and radiomics features in [Mehta et al., 2021], but the biomarkers are not predicted by a computational model and the annotations must be provided when the model is applied to unseen data. Shen et al. [2019] uses DNNs to predict biomarkers, and extract features from previous layers of the biomarker predictor to be used in the malignancy classifier via a jump connection. Those features entering the final malignancy classifier are not interpretable by radiologists. Our evaluation of the best ML classifiers using multiple sets of features helped us to identify a high-performing classifier while maintaining greater interpretability.

2 Methods

2.1 ConRad models and data

The proposed *ConRad* model is designed to extract different aspects of cancer images, leveraging well-established statistical properties and clinical variables of tumors. Particularly, our final model uses biomarkers predicted from a concept bottleneck model (CBM) [Koh et al., 2020] and radiomic features [Hancock and Magnan, 2016] (visualized in fig. 1). CBM-predicted biomarkers and radiomic features are fed to ML classifiers to predict the tumor status (benign vs. malignant). Additionally, we built an end-to-end classifier based on a fine-tuned ResNet model [He et al., 2016] which we use as a baseline comparison.

We particularly focus on CT images of lung tumors from the LIDC-IDRI (Lung Image Database Consortium and Image Database Resource Initiative) dataset [Armato III et al., 2011]. The dataset consists of thoracic CT scans of 1018 cases alongside segmentations, the likelihood of malignancy, and annotated biomarkers for nodules with diameter $> 3\text{mm}$, obtained by up to four radiologists. The CT scans were processed using the `pylidc` package [Hancock and Magnan, 2016], which clusters the nodule annotations¹ and provides a consensus consolidation of the annotated nodule contours. The likelihood of malignancy is ranked from one (highly unlikely) to five (highly suspicious) and we aggregate the radiologists' different annotations by calculating the median, where nodules with a median of three are discarded as ambiguous and above or below three as benign or malignant. This procedure yields a total of 854 nodules, 442 of which are benign.

Input samples were created by first isotropically resampling the CT scans to 1mm spacing and then extracting 32×32 crops around the nodule center in the axial, coronal, and sagittal planes. Hounsfield unit values below -1000 and above 400 were clamped to filter out air and bone regions.

2.2 Feature engineering and Model training

First, we conduct the standard radiomic feature extraction from LIDC-IDRI samples using the `PyRadiomics` package [van Griethuysen et al., 2017]. Particularly, three classes of radiomic features are calculated based on first-order statistics (18 features), 3D shapes (14 features), and higher-order statistics (75 features). All radiomic features are extracted from images where the tumor has been delineated using the segmentation masks provided by the LIDC data. First-order statistics include energy, entropy, centrality, and other distributional values are calculated. Shape features include volumes, areas, sphericity, compactness, elongation, and other descriptors of masked tumors. Higher order statistics are given by the Gray Level Co-occurrence Matrix, Gray Level Size Zone, and others.

Second, a ResNet-50 [He et al., 2016] model pre-trained on the ImageNet [Deng et al., 2009] is fine-tuned to predict eight well-known clinical variables informative of tumors, in a concept bottleneck model (CBM) [Koh et al., 2020].

¹This step is necessary in the presence of multiple nodules in a single scan since the dataset does not indicate which annotations belong to the same nodule. In case `pylidc` assigns more than four annotations to a nodule, the concerned nodule is not admissible.

Instead of predicting the tumor status directly (benign vs malignant), the CBM associates the input samples with annotated biomarkers provided by the LIDC-IDRI dataset; namely, subtlety, calcification, sphericity, margin, lobulation, spiculation, texture, and diameter. The values used for training the CBM are obtained by averaging the annotations provided by the different radiologists.

Note, that the degree to which the described features are interpretable as well as in which way they are interpretable varies. Radiomics features are all interpretable in the sense that they follow from a rather simple mathematical definition. Since many of them represent rather abstract statistical features, their meaning may nonetheless be not intuitive for clinicians. The predicted biomarkers, on the other hand, are computed by an opaque algorithm (the DNN) but their meaning can be immediately understood.

To match the input dimensions of the ResNet-50 model, input samples are upscaled to 224×224 and duplicated in each color channel. Input samples are z-normalized with mean and standard deviation obtained from the training set and identical normalization applied to the test set. We employ 5-fold cross-validation. The model is trained for 50 epochs using the Adam optimizer with PyTorch default parameters and a mini-batch size of 32. The initial learning rate is set to 10^{-3} and is annealed by multiplying with 0.1 after 20 and 40 epochs. During training, an input sample is obtained by randomly selecting one of the three views and during testing, the model output is averaged across all three views to obtain the final output. The trained CBM is used to obtain predicted values for selected biomarkers from samples in the testing set. Unless specified, our evaluation is based on predicted biomarkers (instead of annotated values) to reflect clinical practices where labor-intensive manual segmentation and quantification may be unavailable. Note that we included clinical labels from LIDC-IDRI but depending on the data and domain experts, other biomarkers may be used to train the CBM.

Third, we have also extracted features from training a convolutional neural network (CNN) to directly predict the tumor status. For fair comparison, the same ResNet-50 architecture used in CBM was used to build CNNs. The preprocessing and training procedure is identical to the CBM described above. This end-to-end classifier gives us a baseline to be compared with our proposed interpretable ConRad model. Furthermore, we extract 512 features from the global average pooling layer of the fine-tuned ResNet-50, which are also fused with the radiomics features and CBM-derived biomarkers for downstream classification. We investigate whether a black box DNN model may have superior performance for classifying lung cancer images. And if so, what trade-off between interpretability and accuracy may exist and be acceptable for radiological applications.

2.3 Machine Learning Classifiers

There are three types of features available for training a model to classify the malignancy of nodules. Using each type of features and their combinations, we constructed a total of 7 datasets for the final classifier:

- Biomarkers + Radiomics (ConRad models)
- Radiomics features
- Biomarkers (predicted by CBM)
- CNN features
- CNN + Radiomics
- CNN + Biomarkers
- CNN + Radiomics + Biomarkers (All)

Note that a nodule diameter appears in both Biomarkers and Radiomics feature sets. Having two features that are closely related would cause instability. Thus when necessary, we removed a diameter from Biomarkers. All datasets are z-score normalized on the training set and identical normalization is applied on the test set.

As final-layer classifiers (fig. 1), we applied and evaluated linear and non-linear support vector machine (SVM) [Cortes and Vapnik, 1995], logistic regression [Cox, 1958] with and without Lasso regularization [Tibshirani, 1996], and random forest [Ho, 1995]. The SVM and Lasso regularization parameters C and λ , respectively, are selected via 5-fold cross-validation on the whole dataset. The Lasso (least absolute shrinkage and selection operator) adds L_1 penalty to the loss function, which may achieve feature selection with coefficients of 0. The Lasso has been applied on a large number of radiomic features to remove highly correlated features, such that the optimal model performance is achieved with much less features [Koh et al., 2022]. For each combination of features, we track the number of features selected via the Lasso.

Overall, we built five classifiers using seven aforementioned datasets, combining three types of features. We applied an independent 5-fold cross-validation, where each classifier is trained on four folds and performance is evaluated on the held-out fold. The performance metrics (namely accuracy, precision, and recall) are calculated and averaged across

Table 1: Evaluation of different classifiers in ConRad models. Performance metrics are averaged over the five-fold cross-validation.

Final Layer Classifier	Recall	Precision	Accuracy
Non-linear SVM	0.886	0.899	0.897
Linear SVM	0.886	0.893	0.893
Random Forest	0.879	0.883	0.881
Logistic Regression	0.884	0.893	0.892
Logistic Regression with the Lasso	0.896	0.893	0.896

5-fold cross-validation. A receiver operating characteristic (ROC) curve is constructed by measuring false positive rates (FPR) and true positive rates (TPR) at a wide range of thresholds.

Our proposed model can be contrasted with popular end-to-end DNN algorithms which are considered to be uninterpretable “black box” models. Instead, we are interested in creating an interpretable method, where the final prediction is explained by statistically and clinically relevant features. Furthermore, we leverage and expose oncological knowledge by directly utilizing radiomic features. Importantly, ML classifiers competitively use multiple types of features (radiomics and biomarkers) which helps to highlight their interplay.

3 Results

3.1 Evaluation of ConRad models

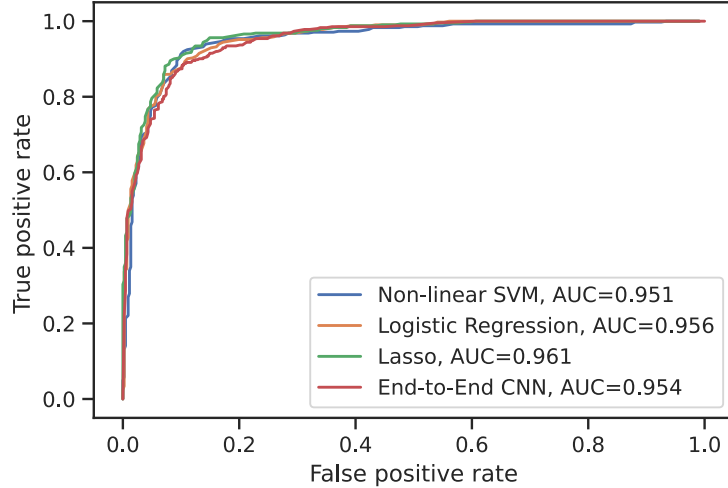


Figure 2: ROC curves for ConRad models in comparison with the end-to-end CNN model. At varying thresholds, false positive and true positive rates are measured for each classifier, followed by averaging over 5 test sets. The areas under the ROC curves (AUCs) are similar in all considered classifiers, where the logistic regression with the Lasso outperforms.

ConRad models combine tumor biomarkers predicted from DNNs and radiomic features defined by radiological experts. LIDC-IDRI contains 8 biomarkers, which are used to construct a concept bottleneck model (CBM) using the pre-trained ResNet-50. We ran each of the CT scan through PyRadiomics to obtain first-order statistics (18 features), 3D shapes (14 features), and higher-order statistics (75 features). We have trained and evaluated five different ML classifiers, based on a total of 115 features.

The model accuracy, recall, and precision are averaged over five-fold cross-validation, where the test set was not used in training. Table 1 shows that all the classifiers are reporting an accuracy in the range of 0.881 – 0.897; non-linear (radial) SVM outperforms all other classifiers, whereas the Random Forest is the worst. For the majority of feature sets, linear SVM performs worse than a non-linear SVM. In terms of the ROC, all the ConRad models and the end-to-end CNN model perform similarly (fig. 2).

When the Lasso (least absolute shrinkage and selection operator) was additionally applied on logistic regression, only 12 out of 114 features (see “Biomarkers+Radiomics” in fig. 3) were selected. The logistic regression with the lasso increased the model performance compared to that without the lasso. Additionally, using a small set of features is inherently more interpretable, as 12 features can be readily visualized and understood.

3.2 Comparison to CNN models

Table 2: Model accuracy of baseline CNN models. Except the first row, all classifiers use CNN features. Compare to table 1.

Classifier	Accuracy
End-to-end CNN classifier	0.891
Non-linear SVM	0.875
Linear SVM	0.87
Random Forest	0.888
Logistic Regression	0.858
Logistic Regression with the Lasso	0.891

In order to compare the ConRad models to baselines, we constructed models that exclusively rely on CNN features, extracted from the end-to-end model outlined in section 2. The end-to-end CNN classifier itself yields 0.891 accuracy and the other considered classifiers lie in the range from 0.858 to 0.891 (table 2). CNN-based classifiers did, therefore, not perform as well as the ConRad models (compare against table 1). What’s more, radiomics and biomarkers are interpretable representing morphological or biological characteristics, whereas CNN features are not interpretable. Note that ConRad does not aim to maximize the model accuracy, and even slightly lower accuracy may be acceptable in exchange for higher interpretability.

However, there is still a concern that uninterpretable CNN features may contain additional information that could increase the ConRad models’ performance. To test this idea, CNN features are added to ConRad models, creating the fullest models (“CNN + Radiomics + Biomarkers”). The five considered ML classifiers are trained on this feature set and performances are measured over five-fold cross-validation (complete results available in Appendix table A1). For all of the classifiers except random forest, adding CNN features on top of the radiomics and biomarkers decreases the accuracy. Table A1 shows that non-linear SVM with predicted biomarkers and radiomics (i.e., ConRad models) slightly outperforms other approaches in terms of precision and accuracy. We also observe that the inclusion of the Lasso improves logistic regression for most feature sets across recall, precision, and accuracy measures.

3.3 The Lasso and Feature Selection

In a regression model, the Lasso [Tibshirani, 1996] adds a L_1 penalty in the loss function which may reduce weights (i.e., coefficients in logistic regression), even to zero. The zero weights imply feature selection, where only a subset of all available features is used in classification. We found that the Lasso drastically reduces the number of considered features in most of the feature sets fig. 3. All 8 biomarkers are automatically selected by the Lasso, presumably due to their low dimension. When considering 2048 CNN features, only 4.10% (84 features) were selected fig. 3.

Logistic regression with the Lasso does not only strongly reduce the number of selected features, but performs comparably or superiorly to the non-regularized logistic regression on almost every considered dataset and performance metric (table A1). On the pure radiomics features, the Lasso selects five shape features, seven higher-order statistics features, and the first-order minimum. With just 12.1% of radiomic features, the accuracy remains the same. When combining biomarkers and radiomics features in the proposed ConRad approach, the Lasso selects five biomarkers and seven radiomics features. Using this subset of features (10.5% of features), the regularized logistic regression achieves 0.896 accuracy, compared to the unregularized version with 0.892 accuracy. Feature selection via the Lasso increases interpretability without losing model performance.

4 Discussion

We investigated different models to classify the lung nodule malignancy, with a focus on interpretability and explainability. Particularly, as feature engineering, a concept bottleneck model (CBM) predicts biomarkers. When applied, the proposed ConRad model does not need annotated biomarkers as often is a case in real world. In total, we investigated 35 classifiers, utilizing seven combinations of features and five ML algorithms. Additionally, an end-to-end CNN classifier

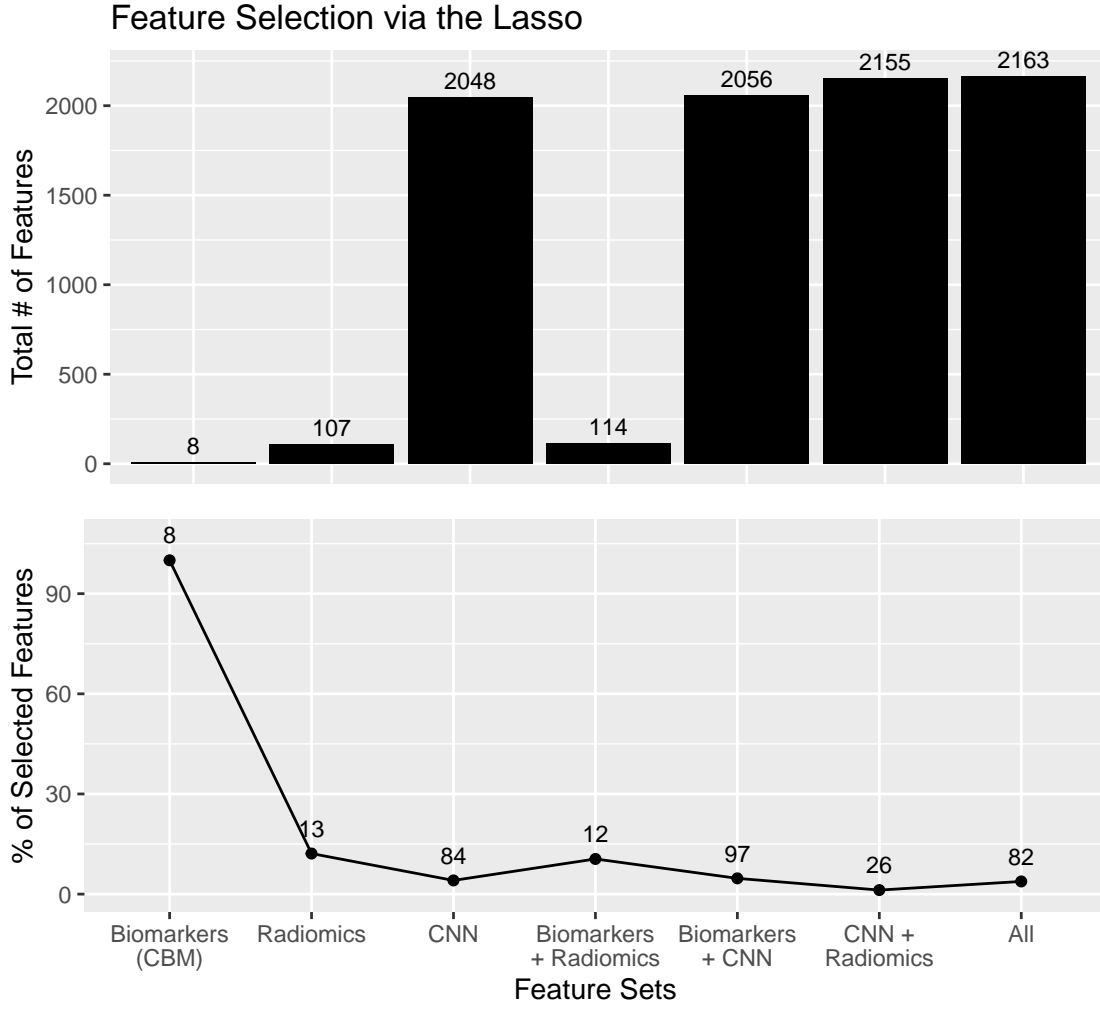


Figure 3: Feature selection by the Lasso in logistic regressions. In each feature set, the Lasso (L_1 regularization) is applied with the penalty parameter selected via cross-validation. Except for biomarkers which only contain 8 features, only small percentages of features are selected.

was evaluated as a baseline. ConRad classifiers based on biomarkers and radiomics features show great performance on par with the end-to-end CNN model, which inherently act as a black box. Non-linear SVM and logistic regression with the Lasso showed the best performance generally.

The intermediate features that feed into the final classifier are interpretable and clinically meaningful by design. The biomarkers represent properties of nodules that have an intuitive meaning for clinicians, who can therefore gain understanding of the decision-making process of the model. This can nurture trust in the ML model since the users don't have to blindly believe the model's classifications. Instead, the users can comprehend, and even interact with, how the model reaches its decisions. For example, if a truly small nodule has been incorrectly predicted to have a large diameter, the clinician may recognize by visually inspecting the CT scan (i.e., a routine tasks). This may allow them to making informed decisions with a support of ML. Furthermore, in the ConRad model, the diameter prediction can be corrected by the clinician, directly resulting in updated prediction. Our ConRad model, therefore, lends itself to a human-in-the-loop (HITL) approach, that may help gaining deeper understanding and trust of the model operating characteristics.

Besides using independent training steps to create an interpretable classifier, we also consider feature selection in malignancy classification. When combining biomarkers and radiomics features, the number of selected features were drastically reduced with the Lasso [Tibshirani, 1996]. Many biomarkers and radiomics features may be correlated, thus removing redundancy can stabilize the model and improve the overall performance with translational potentials

[Koh et al., 2022]. When applied to CNN features, extreme reduction to only 1 – 5% features actually improved the model accuracy. Not only are CNN features unexplainable, a majority of them contain redundant information and do not contribute to the malignancy classification. In the future, this may be a fruitful way to investigate how to identify predictive features, while ensuring interpretability inherent in a manageable number of features.

The combination of biomarkers and radiomics features outperforms all other considered combinations, although the biomarkers demonstrated the most predictive power for the LIDC-IDRI data [Armato III et al., 2011]. Some of the most critical information about lung nodules are contained in both feature sets, as exemplified by a diameter. Thus, we consider both feature sets to be critical part of bringing clinical knowledge into interpretable ML, especially as real world medical images may not contain as rich annotations as LIDC-IDRI. Pre-defined mathematical characterization of medical images in radiomics is always available and clinically validated [Lambin et al., 2017, Yip and Aerts, 2016]. We plan to investigate deeper into the interplay between these features, especially as we plan to apply ConRad to other medical imaging datasets.

Overall, the proposed ConRad model combines concept bottleneck models and radiomics to create an interpretable model, compared to end-to-end DNN classifiers. Transparency and explainability in a model prediction helps radiologists and oncologists to understand and form informed diagnosis and prognosis. Without that critical interpretability component, a black box classifier like end-to-end DNNs may harbor critical failure modes that is unknown and unknowable. Therefore, instead of focusing solely on model performance for medical applications, more investigations that consider interpretability are warranted to see broader incorporation of explainable AI in radiology and oncology.

Acknowledgement

This work was funded by the ERA-Net CHIST-ERA grant [CHIST-ERA-19-XAI-007] long term challenges in ICT project INFORM (ID: 93603), by the National Science Centre (NCN) of Poland [2020/02/Y/ST6/00071]. This research was carried out with the support of the Interdisciplinary Centre for Mathematical and Computational Modelling University of Warsaw (ICM UW) under computational allocation no GDM-3540; the NVIDIA Corporation’s GPU grant; and the Google Cloud Research Innovators program.

References

World Health Organization. Cancer fact sheet. <https://www.who.int/news-room/fact-sheets/detail/cancer>. Accessed: 2023-02-01.

Centers For Disease Control And Prevention. Compressed mortality file 1999-2016 series 20. CDC WONDER On-Line Database <https://wonder.cdc.gov/mortsq1.html>. Accessed: 2023-02-01.

Jeroen Van der Laak, Geert Litjens, and Francesco Ciompi. Deep learning in histopathology: the path to the clinic. *Nature medicine*, 27(5):775–784, 2021.

Riccardo Miotto, Fei Wang, Shuang Wang, Xiaoqian Jiang, and Joel T Dudley. Deep learning for healthcare: review, opportunities and challenges. *Briefings in bioinformatics*, 19(6):1236–1246, 2018.

Cynthia Rudin, Chaofan Chen, Zhi Chen, Haiyang Huang, Lesia Semenova, and Chudi Zhong. Interpretable machine learning: Fundamental principles and 10 grand challenges. *Statistica Surveys*, 16:1–85, 2022.

Philippe Lambin, Ralph T. H. Leijenaar, Timo M. Deist, Jurgen Peerlings, Evelyn E. C. de Jong, Janita van Timmeren, Sebastian Sanduleanu, Ruben T. H. M. Larue, Aniek J. G. Even, Arthur Jochems, Yvonka van Wijk, Henry Woodruff, Johan van Soest, Tim Lustberg, Erik Roelofs, Wouter van Elmpt, Andre Dekker, Felix M. Mottaghy, Joachim E. Wildberger, and Sean Walsh. Radiomics: the bridge between medical imaging and personalized medicine. *Nature Reviews Clinical Oncology*, 14(12):749–762, 2017. doi:10.1038/nrclinonc.2017.141. URL <https://doi.org/10.1038/nrclinonc.2017.141>.

Stephen SF Yip and Hugo JW Aerts. Applications and limitations of radiomics. *Physics in Medicine & Biology*, 61 (13):R150, 2016.

Mathieu Hatt, Catherine Cheze Le Rest, Florent Tixier, Bogdan Badic, Ulrike Schick, and Dimitris Visvikis. Radiomics: data are also images. *Journal of Nuclear Medicine*, 60(Supplement 2):38S–44S, 2019.

Samuel G Armato III, Geoffrey McLennan, Luc Bidaut, Michael F McNitt-Gray, Charles R Meyer, Anthony P Reeves, Binsheng Zhao, Denise R Aberle, Claudia I Henschke, Eric A Hoffman, et al. The lung image database consortium (lidc) and image database resource initiative (idri): a completed reference database of lung nodules on ct scans. *Medical physics*, 38(2):915–931, 2011.

Pang Wei Koh, Thao Nguyen, Yew Siang Tang, Stephen Mussmann, Emma Pierson, Been Kim, and Percy Liang. Concept bottleneck models. In *International Conference on Machine Learning*, pages 5338–5348. PMLR, 2020.

Robert Tibshirani. Regression shrinkage and selection via the lasso. *Journal of the Royal Statistical Society. Series B (Methodological)*, 58(1):267–288, 1996. ISSN 00359246. URL <http://www.jstor.org/stable/2346178>.

Gintare Karolina Dziugaite, Shai Ben-David, and Daniel M Roy. Enforcing interpretability and its statistical impacts: Trade-offs between accuracy and interpretability. *arXiv preprint arXiv:2010.13764*, 2020.

Wei Shen, Mu Zhou, Feng Yang, Caiyun Yang, and Jie Tian. Multi-scale convolutional neural networks for lung nodule classification. In *Information Processing in Medical Imaging: 24th International Conference, IPMI 2015, Sabhal Mor Ostaig, Isle of Skye, UK, June 28-July 3, 2015, Proceedings 24*, pages 588–599. Springer, 2015.

Devinder Kumar, Alexander Wong, and David A Clausi. Lung nodule classification using deep features in ct images. In *2015 12th conference on computer and robot vision*, pages 133–138. IEEE, 2015.

Wentao Zhu, Chaochun Liu, Wei Fan, and Xiaohui Xie. Deeplung: Deep 3d dual path nets for automated pulmonary nodule detection and classification. In *2018 IEEE winter conference on applications of computer vision (WACV)*, pages 673–681. IEEE, 2018.

Mundher Al-Shabi, Hwee Kuan Lee, and Maxine Tan. Gated-dilated networks for lung nodule classification in ct scans. *IEEE Access*, 7:178827–178838, 2019.

Mundher Al-Shabi, Kelvin Shak, and Maxine Tan. Procan: Progressive growing channel attentive non-local network for lung nodule classification. *Pattern Recognition*, 122:108309, 2022.

Jason L Causey, Junyu Zhang, Shiqian Ma, Bo Jiang, Jake A Qualls, David G Politte, Fred Prior, Shuzhong Zhang, and Xiuzhen Huang. Highly accurate model for prediction of lung nodule malignancy with ct scans. *Scientific reports*, 8(1):9286, 2018.

Kushal Mehta, Arshita Jain, Jayalakshmi Mangalagiri, Sumeet Menon, Phuong Nguyen, and David R Chapman. Lung nodule classification using biomarkers, volumetric radiomics, and 3d cnns. *Journal of Digital Imaging*, pages 1–20, 2021.

Shiwen Shen, Simon X Han, Denise R Aberle, Alex A Bui, and William Hsu. An interpretable deep hierarchical semantic convolutional neural network for lung nodule malignancy classification. *Expert systems with applications*, 128:84–95, 2019.

Matthew C Hancock and Jerry F Magnan. Lung nodule malignancy classification using only radiologist-quantified image features as inputs to statistical learning algorithms: probing the lung image database consortium dataset with two statistical learning methods. *Journal of Medical Imaging*, 3(4):044504–044504, 2016.

Kaiming He, Xiangyu Zhang, Shaoqing Ren, and Jian Sun. Deep residual learning for image recognition. In *Proceedings of the IEEE conference on computer vision and pattern recognition*, pages 770–778, 2016.

Joost J.M. van Griethuysen, Andriy Fedorov, Chintan Parmar, Ahmed Hosny, Nicole Aucoin, Vivek Narayan, Regina G.H. Beets-Tan, Jean-Christophe Fillion-Robin, Steve Pieper, and Hugo J.W.L. Aerts. Computational Radiomics System to Decode the Radiographic Phenotype. *Cancer Research*, 77(21):e104–e107, 10 2017. ISSN 0008-5472. doi:10.1158/0008-5472.CAN-17-0339. URL <https://doi.org/10.1158/0008-5472.CAN-17-0339>.

Jia Deng, Wei Dong, Richard Socher, Li-Jia Li, Kai Li, and Li Fei-Fei. Imagenet: A large-scale hierarchical image database. In *2009 IEEE conference on computer vision and pattern recognition*, pages 248–255. Ieee, 2009.

Corinna Cortes and Vladimir Vapnik. Support-vector networks. *Machine learning*, 20(3):273–297, 1995.

David R Cox. The regression analysis of binary sequences. *Journal of the Royal Statistical Society: Series B (Methodological)*, 20(2):215–232, 1958.

Tin Kam Ho. Random decision forests. In *Proceedings of 3rd international conference on document analysis and recognition*, volume 1, pages 278–282. IEEE, 1995.

Dow-Mu Koh, Nickolas Papanikolaou, Ulrich Bick, Rowland Illing, Charles E Kahn Jr, Jayshree Kalpathi-Cramer, Celso Matos, Luis Martí-Bonmatí, Anne Miles, Seong Ki Mun, et al. Artificial intelligence and machine learning in cancer imaging. *Communications Medicine*, 2(1):133, 2022.

Appendix

Table A1: Full comparison of five classifiers on 7 different combinations of features. Performance metrics are averaged over the five-fold cross-validation.

Classifier	Features	Recall	Precision	Accuracy
Non-linear SVM	cnn	0.869	0.880	0.875
	radiomics	0.869	0.873	0.876
	biomarkers	0.900	0.876	0.890
	all	0.869	0.886	0.879
	cnn+rad	0.869	0.878	0.876
	bio+rad	0.886	0.899	0.897
	bio+cnn	0.876	0.868	0.891
Linear SVM	cnn	0.859	0.862	0.870
	radiomics	0.879	0.880	0.883
	biomarkers	0.891	0.893	0.896
	all	0.855	0.870	0.863
	cnn+rad	0.864	0.873	0.868
	bio+rad	0.886	0.893	0.893
	bio+cnn	0.852	0.861	0.869
Random forest	cnn	0.871	0.887	0.888
	radiomics	0.876	0.878	0.878
	biomarkers	0.891	0.879	0.889
	all	0.881	0.897	0.885
	cnn+rad	0.874	0.894	0.890
	bio+rad	0.879	0.883	0.881
	bio+cnn	0.891	0.889	0.890
Logistic regression	cnn	0.857	0.858	0.858
	radiomics	0.874	0.884	0.883
	biomarkers	0.886	0.892	0.893
	all	0.871	0.878	0.875
	cnn+rad	0.864	0.864	0.874
	bio+rad	0.884	0.893	0.892
	bio+cnn	0.850	0.867	0.874
Logistic regression with the Lasso (feature selection)	cnn	0.871	0.876	0.891
	radiomics	0.876	0.881	0.883
	biomarkers	0.886	0.895	0.895
	all	0.886	0.882	0.895
	cnn+rad	0.871	0.894	0.888
	bio+rad	0.896	0.893	0.896
	bio+cnn	0.874	0.883	0.889